Waste and Biomass Valorization
https://doi.org/10.1007/s12649-022-01863-1

ORIGINAL PAPER

A New Insight Into the Anti Proliferative and Apoptotic Effects of Fulvic and Humic Acids as Bio Product of Humus on Breast Cancer Cells, Optimized by Response Surface Methodology

Leila Zolghadr[1] · Gholamreza Rezaei Behbehani[1] · Babak Pakbin[2] · Seied Ali Hosseini[3] · Nematollah Gheibi[4]

Received: 30 November 2021 / Accepted: 26 June 2022

Abstract

Today, plant compounds and substances of natural origin as bio products are strongly recommended for the prevention and treatment of cancer. In the field of biomedicine anti-viral, anti-inflammatory, anti-oxidant properties among the most known activities of Humus and the products obtained from humus. In this study, the effect of humic and fulvic acids (HA, FA), bio product of humus, on breast cancer cells (MCF7), the most common cancer among women, was investigated. To achieve optimum cytotoxic time and determine the effect of the different parameters the Response Surface Methodology (RSM) was applied. The main parameters influencing the cytotoxic performance in the MTT assay, such as time and concentrations were regarded. The cell viability was measured using different concentrations of HA and FA including 10, 50, 100, and 200 µg/mL for 14, 24, and 48 h, respectively. Apoptosis, cell cycle, mechanical properties and survivin gene expression of MCF7 cells treated with HA and FA were analyzed after 14 h. Our results showed that HA and FA induced apoptosis, reduced cell viability and gene expression in the cured MCF7 cells. We have seen a dose-dependent behavior of HA in increasing the cell population in phase Sub-G1. The results of AFM showed that the increasing behavior of elastic modulus value and cell–cell adhesion forces were dose-dependent in cells treated with HA and FA. The golden result of this study was the matching of laboratory and statistical results which confirms the success of the RSM model in biological researches.

✉ Gholamreza Rezaei Behbehani
grb402003@yahoo.com

✉ Nematollah Gheibi
gheibi_n@yahoo.com

Leila Zolghadr
L.zolghadr60@gmail.com

Babak Pakbin
babak.pakbin@gmail.com

Seied Ali Hosseini
sahosseini@eng.ikiu.ac.ir

[1] Department of Chemistry, Faculty of Science, Imam Khomeini International University, P. O. Box.288, Qazvin 34149, Iran

[2] Medical Microbiology Research Center, University of Medical Sciences, Qazvin, Iran

[3] Electrical Engineering Department, Faculty of Engineering, Imam Khomeini International University, Qazvin, Iran

[4] Cellular and Molecular Research Center, Research Institute for Prevention of Non-Communicable Diseases, Qazvin University of Medical Sciences, Qazvin, Iran

Published online: 17 August 2022

Graphical abstract

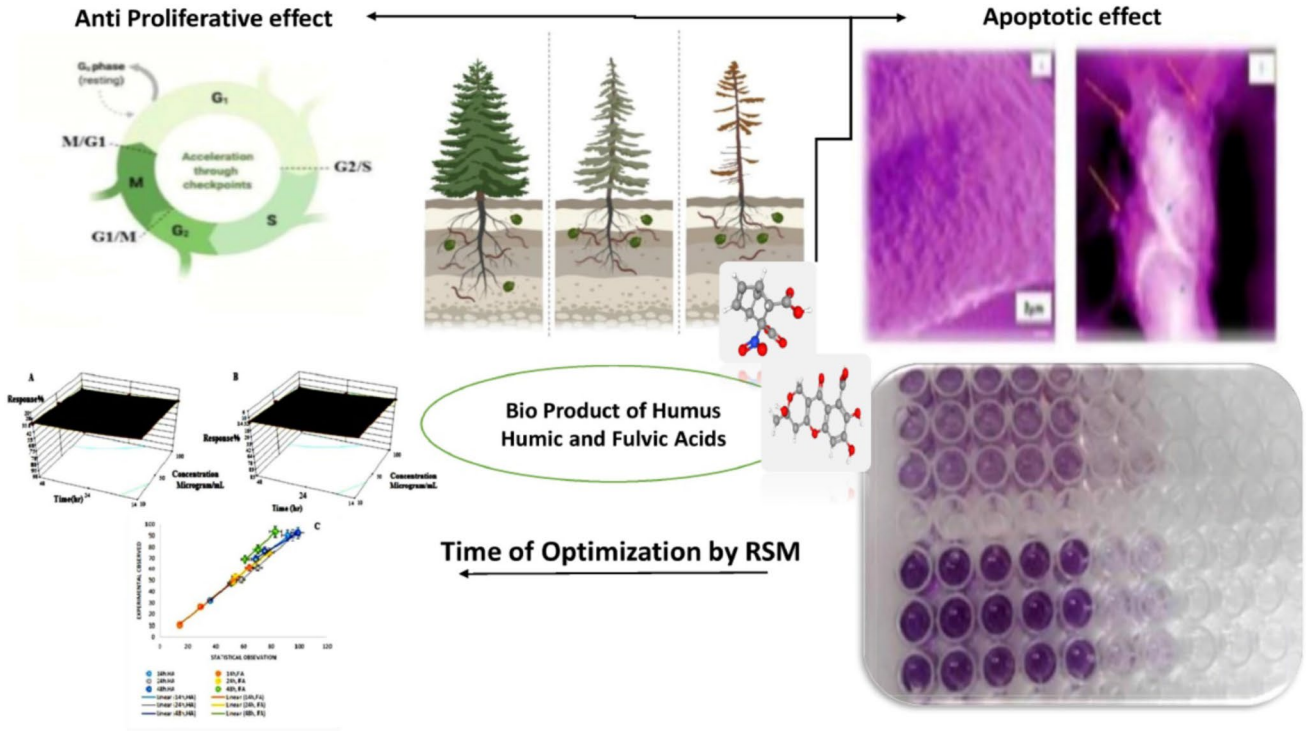

Keywords Bio product · Apoptosis · Breast cancer cell · Response surface methodology · Modulus coefficient

Abbreviations

MCF7	Breast cancer cell line
RSM	Response surface model
FA	Fulvic acid
HA	Humic acid
MTT	3-(4,5-Dimethylthiazol-2-yl)-2,5 diphenyl tetrazolium bromide
AFM	Atomic Force Microscopy

Statement of Novelty

The effect of humic and fulvic acids as bio stimulants in agriculture has been proven. The current research aimed to examine the anticancer attributes of biopolymers extracted from soil. Another advantage of this study over other studies in the field of cancer is the combination of experimental tools and statistical tools for optimization. It seems that the optimal time presented in this study can help researchers in this field, because the effectiveness of drugs in a short time and fewer side effects are more beneficial to patients.

Introduction

Today, more than 2/3 of anticancer drugs worldwide are derived from plant metabolites [1]. These plant compounds have anticancer potential and are found in foods such as fruits and vegetables. Among the plant metabolites, most cancer-related researches have been done on the flavonoid family compounds [2]. Along with herbal ingredients, another significant source of anticancer drugs in healthful foods and plants are natural organic substrates. Humic substances (HS) are commonly found in decaying organic matter including plants, animal residues, sewage and soil. utilization of HS, composed of humic (HA) and fulvic acid (FA), has been recognized as a long run product since the 1980s [3]. Humus and the products obtained from humus are used in agricultural and biomedical fields. The HA, a type of polymer including macromolecules that has a high molecular weight, is obtained from decomposing organic matter [4]. In HA, aromatic rings and groups of alkoxyl, carboxyl, quinone carbonyl, ketonyl, and phenolic hydroxyl are responsible for most anticancer properties [5]. However,

HA, due to some functional groups such as carboxyl, phenol, quinone showed intense antioxidant activity [6].The HA is degraded by microbial reactions, oxidation, and reduction, producing resorcinol, meta- and ortho-phthalic acids, and different phenolic compounds [5, 7]. Another compound that is an attractive candidate in many pharmaceutical studies due to its structure and active groups is FA [8]. The FA is an admixture of complex polymers with active functional groups [9]. FA, used as a supplement, contains active functional groups of phenolic hydroxyl, ketone carbonyl, quinone carbonyl, carboxyl, and alkoxyl and aromatic rings that mediate absorbing several necessary nutrients into the body [10]. Several reports confirm the antimicrobial and anti-inflammatory properties of FA [11, 12]. Several studies have demonstrated the anticancer properties of HA and FA [13, 14], and its biological significance recognized for several years, there is still minimal scientific understanding the claims of its biological properties. Breast cancer is the most prevalent cancer and the first cause of mortality in women aged 44 and over in the world. Also, this cancer is responsible for about 19% of cancer-related deaths [15–17]. According to the world health organization, about 1.3 million females around the world are diagnosed with breast cancer yearly. After lung cancer, the highest mortality is related to this type of cancer. The highest death rate from breast cancer in 2014–2017 were observed in Madison County, Mississippi (the mortality rate of 52 individuals per 100,000). The lowest death rate was in Presidio County, Texas (the mortality rate of 15 individuals per 100,000) [18]. The mainstays of treatment and control of breast cancer are surgery (mastectomy), Radiation therapy, and systematic treatments such as chemotherapy, immunotherapy, and thermo-chemotherapy [19]. Despite the radical mastectomy surgeries, only 50% of the patients' rescue [20]. Chemotherapy also has many side effects and can have strong cytotoxic effects on the body's healthy cells [21]. So far, each type of chemotherapy drug was effective only on a limited percentage of the patients. For example, Tamoxifen has been effective in 1/3 of breast cancer patients. Several studies have shown that a proper diet can prevent up to 30% of cancers in some cases [22]. The most critical limitation in cancer treatment has been the cancer cells' resistance against drugs. This limitation can be due to the resistance of the Dotti tumor cells to the drug or chemotherapy and their function is such that resistant cells are chosen from heterogeneous ones. Therefore, by increasing the resistant cells, the healing procedure becomes more challenging. Therefore, choosing suitable drugs having fewer side effects is a priority in the treatment of cancers. One functional mechanism of anticancer medications is inducing apoptosis, causing cancer cells death.

The current research aimed to examine the anticancer attributes of biopolymers extracted from soil (HA and FA) on MCF7 cells. Consequently, we will optimize the time of treatment exposure on cell viability and this optimization will be performed using the RSM. Finally, the selected time's correctness is determined by evaluation of apoptosis, cell cycle, physical properties of cells by atomic force microscopy (AFM), and survivin gene expression.

Materials and Methods

Preparing HA and FA

Preparation and purification process of HA was done based on the protocols described by Ting et al. [23]. Also, the extraction of FA from Humus was conducted by using the base-acid extraction method [24]. Lastly, stock solutions (HA and FA) were prepared at 10, 50, 100, and 200 µg/mL concentrations.

Cell Culture

The researchers supplied a Human breast adenocarcinoma (MCF-7) cell line through Pasteur Institute (Pasteur In., Iran). Then, they activated MCF7 cells in cell culture medium of DMEM, supplemented with 10% (v/v) FBS, with incubation at 37 °C and 5% CO2 and modified the medium every other day. Researchers routinely sub-cultured the cells whenever they were 80% confluent, using 0.25% trypsin–EDTA solution (Biochrom, L2143). When enough cells were obtained, an inverted microscope (Optika IM-3) was used to monitor regularly the proliferation, passages, and tracking of the cells. They removed the cells from the flasks when were confluent, by applying the solution of trypsin–EDTA. Next, they transferred the cells to 96 well Microplates. Cells treated with HA and FA dilutions and the control sample were harvested.

Cell viability Assessment

To investigate the viability of cured cancer cells the 3-(4,5-dimethylthiazol-2-yl)-2,5 diphenyl tetrazolium bromide (MTT) was applied. HA and FA were diluted in the culture medium at five various concentrations of 10, 50,100, and 200 µg/mL. At first, the cell suspension preparation was done at 3000 cells per well in a 96-well plate. MCF-7 cells were cured with definite concentrations for 14, 24, and 48 h and were incubated at 37 °C for 4 h. In the following, after removing the MTT solution, 100 µl of DMSO was added to every well and incubated for 15 min. To assess the absorption of the each well the micro Plate Reader (Biotek, USA)

device was employed [25, 26]. Using the following equation, the cell viability was calculated.

$$\text{Cell Viability}(\%) = \frac{\text{Absorbance of Control} - \text{Absorbance of HA or FAtreated Cells}}{\text{Absorbance of Control}} \times 100 \quad (1)$$

Apoptosis and Cell Cycle Analysis

In analyzing apoptosis and cell cycle phases of the treated cancer cells the flow cytometry was used. The apoptosis of treated MCF7 cells was evaluated using a flow cytometer device (Dickinson Immunocytometry System, CA, USA) and a Bioscience cell apoptosis kit (Ebioscience, San Diego, USA) containing Annexin V-FITC staining and propidium iodide (PI). According to the cell apoptosis kit protocol, cells were seeded in microplate wells and treated in two selective IC50 and 100 µg/mL value concentrations of HA and FA. We allowed the cells to incubate at 37° C for 14 h. After harvesting the cells, phosphate saline buffer (PBS) was used to wash them. The harvested cells' set with Annexin V-FITC and PI for 30 and 5-min, respectively, was performed. Finally, the flow cytometry device was used to measure the expression of Annexin V-FITC and PI. We also evaluated the cell cycle. Floating and adherent cells were pooled and then washed using ice-cold PBS. In the following, after fixing in the solution of PBS-methanol (1:2 v/v), eventually, they were stored at 4◦C for at least 18 h. After rinsing with PBS twice more, the cell pellet was stained using the solution of a fluorescent probe comprising PBS, 40 g/mL of PI, and 40 g/mL of DNase-free RNaseA for 30 min in the darkness and at room temperature. DNA fluorescence of the PI-stained cells was examined through exciting at 488 nm and monitoring by a 630/22 nm bandpass filter employing a flow cytometer of Becton–Dickinson FACS-Calibur. At least 10,000 cells in each sample were analyzed. To estimate the percentage of cells in different cell cycle phases the DNA histograms were more analyzed applying Modfit LT 3.2 software.

Extraction of RNA, Synthesis of cDNA, and Expression of Gene

Expression of survivin gene was measured for viability evaluation of MCF7 cells treated with HA and FA. Reverse transcriptase real-time PCR coupled to $2^{-\Delta\Delta Ct}$ method was used to express the survivin gene in treated (with IC50 and 100 µg/mL value concentrations of HA, FA) and control MCF7 cells. According to the protocol the RiboEx total RNA extraction kit was used to extract the total RNA of cells harvested (GeneAll Biotechnology Co., Korea). Reverse transcription of the extracted RNA was performed using the GeneAll cDNA synthesis kit (GeneAll Biotechnology Co., Korea) and ABI PCR thermal cycler machine model 9092 (Applied Biosystems, USA). The qRT-PCR SYBR green master mix (Ampliqon, Denmark) with the Rotor Gene real-time PCR machine 6000 (Qiagen, USA) were used to perform the Real-time PCR. In every reaction tube, there was 25 µl reaction mix containing 0.5 µl of each primer (10 µM/µl), 12.5 µl supermix kit, and 1 µl cDNA template and sterilized deionized water to the ultimate reaction volume. Researchers used the primers of GAPDH (glyceraldehyde 3-phosphate dehydrogenase) as internal controls. Primer sequences synthesized by SinaColon (SinaColon Co., Iran) have been described as following: Survivin forward 5′- GCCTCCTCTCCTACTTTG-3′ and reverse 5′-CTCAGC CCATCTTCTTCC-3′; Bax forward 5′TGGGAAGTTTCA AATCAGC-3′ and reverse 5′-TGGGAAGTTTCAAATCAG C-3′, Bcl_2 forward 5′-CAATGACCCCTTCATTGACC-3′, reverse 5′-TGGAAGATGGTGATGGGATT-3′. As primary denaturation, the qRT-PCRs were carried out at 95 °C for 15 min, followed by 40 cycles, including 15 s at 95 °C and 1 min at 60 °C.Also, the caspase-3 gene primers forward AAGCGAATCAATGGACTCTGG and reverse CTGTAC CAGACCGAGATG TC was used in study [27, 28]. The cDNA samples were subjected to quantitative PCR in a light cycler apparatus (Rotor-Gene6000, Qiagen, USA) with 40 cycles consisting of 94 °C for 15 s, 58 °C for 30 s, and 72 °C for 30 s. Melting curve analysis was performed from 60 to 95 °C to assess the specificity of PCR products. When the cycle threshold (C_t) for each reaction was determined, then, the $2^{-\Delta\Delta Ct}$ method was used to measure relative gene expressions [29].

Atomic Force Microscopy (AFM) Analysis

Initially, researchers seeded MCF7 cells in Petri dishes and put them into a CO_2 Incubator device at 37 °C. Then cells were cured by 50 and 100 µg/mL of FA and HA. After 14 h, the washing process was done by PBS. Then, the cell fixation process was performed for 1 min with 0.5% Glutaraldehyde solution. The Glutaraldehyde solution was removed and the process of cell washing continued for 5 min with three replications with PBS. In the last step, after the removal of the buffering, the Petri dishes were dried at room temperature. Nanowizard-2 AFM (JPK Instruments) was used to evaluate the treated cells' elastic behavior. An AFM installed on an inverted optic microscope was mounted to a camera. A V-shaped high sensibility Tip (MIKROMASCH-NSC15/AIBS) with nominal spring constant 0.07–0.35 N/m, 10 nm radius, and side angle 10°, was mounted to the stand. The morphology and ultrastructure of cells were examined in non-contact mode at T:37 ± 2 °C (PetriDishHeater, JPK Instrument). Moreover, standardization methods such as ISO 5725, ISO/IEC 17,042, and ASTM E691 were used for

quality control of images. This equation was also employed in calculating the young's modulus:

$$F = \frac{2}{\pi} \tan(\alpha) \frac{E}{1-\nu^2}\delta^2 \quad (2)$$

F Loading force, E Young's modulus, ν Poisson ratio @ 0.5 is appropriate for cells, δ Indentation, α Half opening angle of a conical tip [30].

Statistical Analysis

The differences between the groups of treatment and control were compared using one–way analysis of variance. The calculation of meaningful differences among data groups was performed applying Duncan's multiple range test and SPSS software version 20 (SPSS®, Armonk, NY, USA). The t-test, F-test, and Z-scores in SPSS and JPK software were applied in the process of the AFM data analysis. The Graphpad Prism8 software was used to draw graphs. The significant level for data was considered less than 0.05.

Optimization Methodology Using the Statistical Tools

Response Surface Methodology was done for optimization in this study via applying the Design–Expert package version 10.0.3.1 (Stat-Ease Inc., Minneapolis, USA) software. RSM was employed in estimating the mathematical relationship between a set of processes as variables and response as a function of the variables and analyzing the impact of different parameters on the cells' cytotoxicity. The impact of independent variables was examined using a 3^2 full factorial design. Drug concentration (X_1) and time (X_2) in this statistical model, including interactive and polynomial terms, were independent variables, while Cell Viability (%) was a dependent one. The coded mathematical model for 3^2 factorial designs is given:

$$Y = b_0 + b_1X_1 + b_2X_2 + b_{12}X_1X_2 + b_{11}X_{12} + b_{22}X_{22} \quad (3)$$

Here that Y is the dependent variable, b_0 is the arithmetic mean response of the nine runs, and b_i is the predicted coefficient for the factor X_i. Whenever two factors synchronically change, the interaction terms (X_1X_2) display how to change the response. The polynomial terms (X_{12} and X_{22}) were included to study non-linearity.

Results

Optimization of Treatment

In this study, we used RSM for optimizing the treatment time of cancer cells with drugs. In previous studies, cytotoxicity of FA and HA at different concentrations after 24, 48, and 72 h was investigated [31–34]. To prepare stock solutions, HA was first dissolved in 1 N NaOH solution (pH > 10), and any undissolved material was removed by filtration. The solution was then acidified with 1 N HCl (pro-analysis grade, Merck, Darmstadt, Germany) to a pH < 2.0 to precipitate the HA, and dissolved metals which bind with HA. Any precipitate formed was collected by centrifugation at 3000×*g* for 30 min, and redissolved in 1 N NaOH. The alkaline-acid treatment was repeated three times to obtain the purest HA. After the third round of acid precipitation, the precipitate was dis-solved in 0.1 N NaOH, and the pH of the resulting solution was adjusted to 7.2–7.4. Also, extraction of FA was conducted from Humus by base-acid extraction methods. Briefly, humus was extracted by

Table 1 Optimal time results of drug effect (HA and FA) on MCF7 cells using RSM

	Variables level		Coded independent variable levels		% Response HA	%Response FA
	X1	X2	A	B		
1	− 1	− 1	10	14	91.48	64.23
2	− 1	0	10	24	95.32	78.33
3	− 1	1	10	48	98.72	82.8
4	0	− 1	50	14	50.99	28.82
5	0	0	50	24	70.08	54.32
6	0	1	50	48	75.32	70.32
7	1	− 1	100	14	35.8	14.32
8	1	0	100	24	58.3	52.3
9	1	1	100	48	68.93	60.95

*X1*drug concentration (µg/m L): Low (10), Mid(50), High(100), *X2* Time (h): Low (14), Mid (24), High (48), Low = -1, Mid = 0, high = 1, *A* Drug Concentration, *B* Time, Response %Cell viability

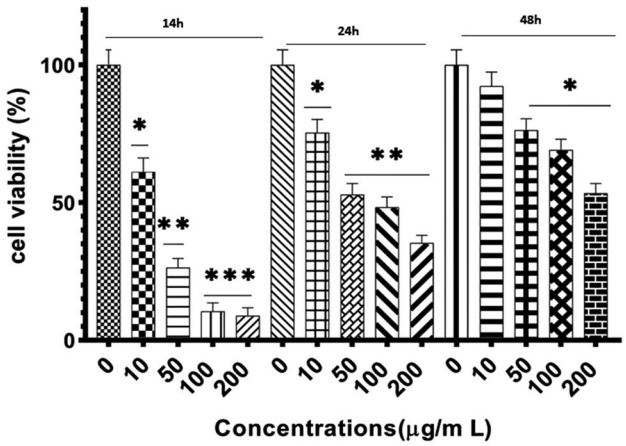

Fig. 1 The MTT assay results in treatment with 0-200 µg/mL concentrations of Humic acid for 14, 24 and 48 h. (P-Value < 0.05*/ < 0.01**/ P-Value < 0.001***)

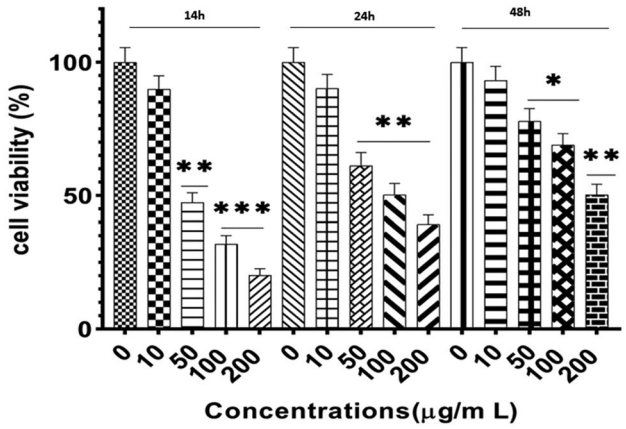

Fig. 2 The MTT assay results in treatment with 0-200 µg/mL concentrations of Fulvic acid for14, 24 and 48 h (P-Value < 0.05/ < 0.01**/ P-Value < 0.001***)

treating with 0.1 M NaOH alkaline solution, filtering, and removing insoluble humic acid. Then, the residual solution was acidified to pH 1 ~ 2 using 6.0 M HCl to yield FA. The precipitated FA was centrifuged to produce FA fractions at 4500×*g* for 30 min. The purified HA and FA were then freeze-dried to a powder form. To optimize the efficiency of the drug regarding three different concentrations and times, we examined the cell viability percentage. The results were obtained after 9 replications with Design–Expert package version 10.0.3.1 (Stat-Ease Inc., Minneapolis, USA) software (Table 1). After obtaining the appropriate times using the computational model, these results were also evaluated in the experimental section. The HA and FA at concentrations of 10, 50, 100, and 200 µg/mL were used to treat MCF-7 cells, for 14, 24, and 48 h. The Cell Viability was significantly affected by FA and HA at the concentrations of 10, 50, 100, and 200 µg/mL (Figs. 1 and 2). Therefore, it was clear that treatments after 14-, 24-, and 48-husing HA and FA were at concentrations ranging from 10 to 200 µg/mL. Our results indicated that, the effect of HA and FA toxicity at 14, 24, and 48 h were observed in the highest toxicity and best efficiency at 50 and 100, and 200 µg/mL, respectively, and according to the selected concentrations of the statistical model, we set the continuation of experiments at 14 h and a concentration range of IC50 and one concentration higher (100 µg/mL). The anticipated response (Y_1) of the process to the independent variables have been provided graphically in 3D space to facilitate the visualization of the response surface's shape in Fig. 3. The effect of time and concentration on Cell viability % is shown in plots A and B, Fig. 3. It is seen from plots A and B that there are significant effects of time and concentrations in the scope of the parameter levels examined. The results show that by decreasing the time and increasing the concentration of viability of cells, it is also decreasing Fig. 3, C; shows the predicted values and experimental values of the Cell viability. High values of $R^2 = 1$ and $R^2 = 0.9918$ for (HA and FA, 14 h), $R^2 = 0.9993$ and $R^2 = 0.9976$ (HA & FA, 24 h), $R^2 = 0.8998$ and $R^2 = 0.9912$ (HA and FA, 48 h) indicated that the model was successful in correlating the response to the studied parameters. Finally, these concentration ranges (50 and 100 µg/mL) and time (14 h) were employed in all following experiments.

Effect of HA and FA on MCF7 Cell Apoptosis

The results of flow cytometry, including Annexin V/PI staining assay for apoptosis analysis of cured and control MCF7 cells after 14 h, are shown in Fig. 4a, b(a–e). The necrotic, late apoptosis, early apoptosis, and live cell ratios were appointed in Q1, Q2, Q3, and Q4 quadrants, respectively. Also, total apoptotic cell ratios were determined (Q2 + Q3) [35]. Cell apoptosis in cured MCF7 cells was computed 26.5, 15.95, 23.9, and 17.84 in HA and FA (100, 50 µg/mL) after 14 h, respectively. Figure 4a, b(a–e). The overall effect of drugs on MCF7 cell lines confirmed late apoptosis induction.

Impact of HA and FA on MCF7 Cell Cycle

Besides, to measure the fluorescence of PI binding to DNA, the profile of the DNA content of HA and FA cured MCF7 was achieved applying flow cytometric analysis. It was ascertained that at which phase HA and FA-induced growth inhibition occur in the cell cycle progression in MCF7, by cellular distribution in various phases at 0, 4, 8, and 14 h of HA and FA (50, 100 µg/mL) treatments. Table 2 and Fig. 5 (A-R) indicated that HA and FA (100 µg/mL) treatments led to a continuous and stable accumulation of cells in the G1 phase that was also

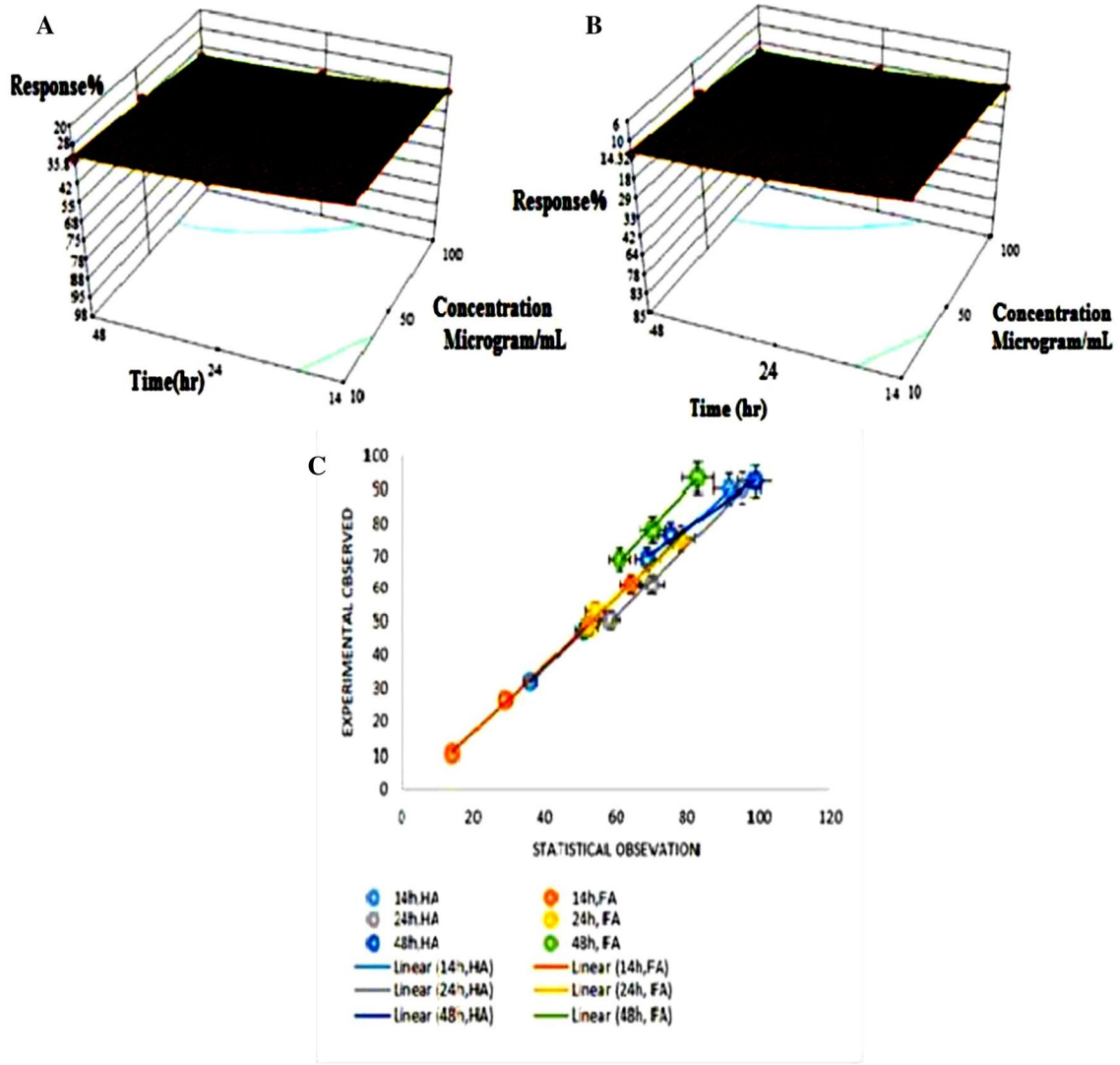

Fig. 3 The response surface plot representing the effect of time and concentrations drug (**a** HA and **b** FA) on the MCF7 Cells. **c** Matching the experimental and statistical results (RSM) of the effect of drugs at14, 24, 48 h

dependent to time. The results of current study suggested that the reduction of viability observed in MCF7 after HA and FA treatments could be due to cell cycle arrest in the G1 phase. Table 2 shows evident changes among groups of control and treatment. These findings stated that HA and FA affected the growth of MCF7 cells at a concentration of 100 µg/mL. Furthermore, no accumulation of G2 populations was observed in treatment with HA and FA. Also, treatment increased the cell cycle retardation degree. Moreover, there was a more increase in the Sub-G_1 population in treatment with HA (50 and 100 µg/mL) and dose-dependent behavior was confirmed by the results of the analysis, but in the case of FA, we could not reach the correct conclusion in phase Sub-G_1, and only at a concentration of 50 µg/ml did we see time-dependent behavior in population growth. Besides, the percentage of MCF7 cells reduced in the S phase when the concentration of FA and HA increased. After treatment with FA and HA at a time of 0–14 h the cells' percentage in the S phase reduced to $16.57 \pm 1.8\%$, $9.42 \pm 0.4\%$ in FA (50 and 100 µg/mL) which was notably less than those of the control group $30.59 \pm 2.5\%$, $32.57 \pm 1.8\%$. There was also a significant decrease in HA with concentrations of 50 and 100 µg/mL compared to the control group in phase S. ($34.62 \pm 2.3\%$, $29.31 \pm 1.6\%$ to $22.32 \pm 3.2\%$, $11.96 \pm 0.2\%$ respectively. The results of phase S analysis confirm the time and dose-dependent behavior.

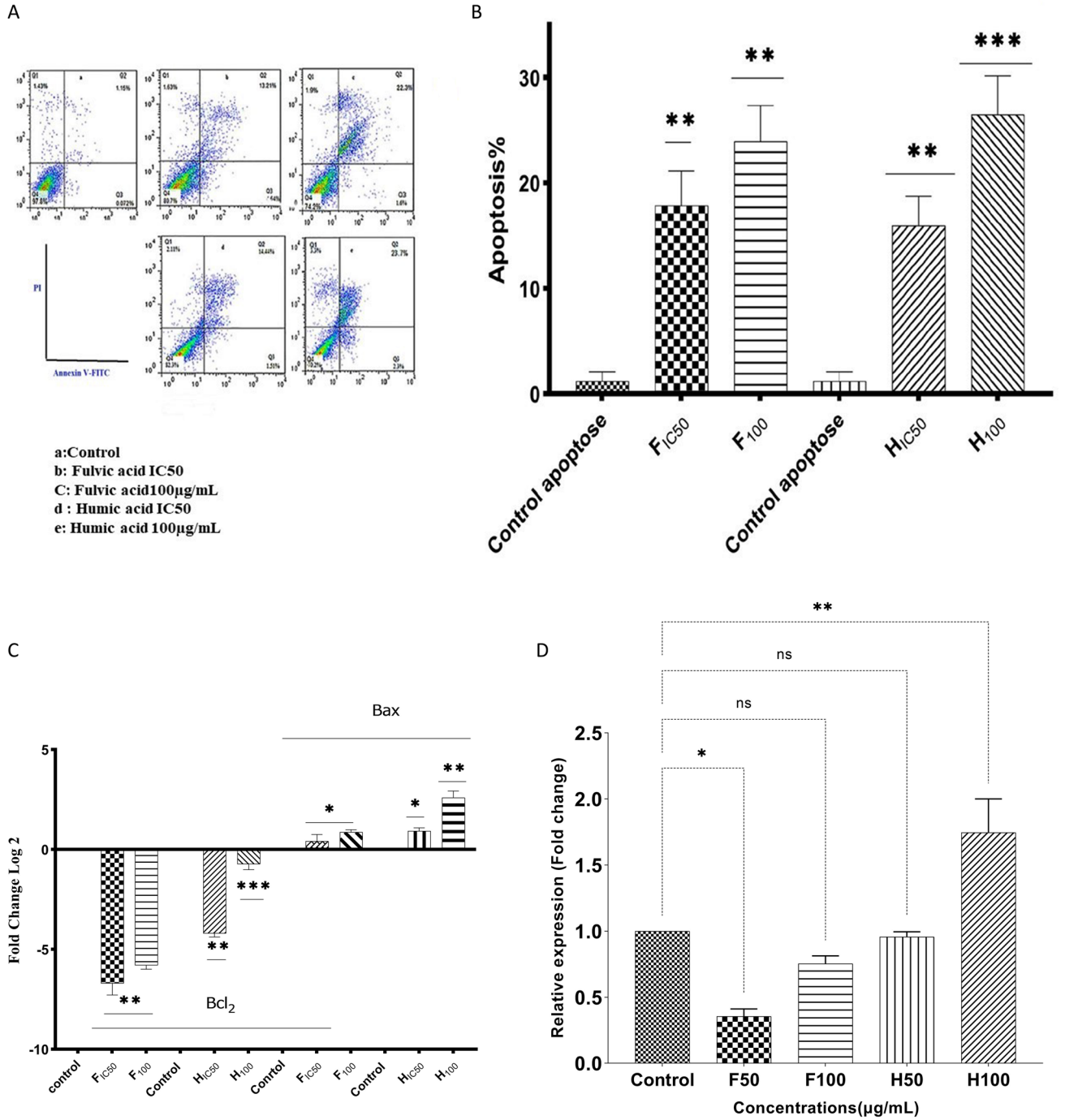

Fig. 4 **a** Apoptosis and necrosis percentage of MCF7 cells based on the flow cytometry assay in treatment with50 and 100 µg/mL concentrations HA and FA for 14 h. (P-Value < 0.05*/< 0.01**/< 0.001***). **b** The flow cytometry assay results in cell treatment with (a): Control, (b): FA 50 µg/ mL, **c** FA 100 µg/mL, **d** HA 50 µg/mL and e: HA 100 µg/mL for 14 h. It shows parts of the flowjo software results. c: The gene expression BAX and BCL_2 in MCF-7 breast cancer cell line treated with concentrations of HA and FA acids (50 and 100 µg/m L) for 14 h, (P-value < 0.05*/< 0.01**/< 0.001***). d: The relative expression level of *caspase-3* gene in MCF-7 breast cancer cell line treated with concentrations of HA and FA acids (50 and 100 µg/mL) for 14 h, (P-value < 0.05*/< 0.01**/< 0.001***). **e** The Atomic Force Microscopy images of the cytoplasmic membrane of MCF7 cells treated with concentrations of HA and FA acids (50 and 100 µg/mL) for 14 h, (A). Control, (B). FA (50 µg/mL), (C). FA (100 µg/mL), (D). HA (50 µg/mL), (E). HA (100 µg/mL) were shown. The blue arrows show the highest elastic modulus areas. The image resolution value was 0-45 µm. (G and F). View of membrane changes and induction of Apoptosis HA (50 and 100 µg/mL) (H). The Youngs' Modulus values of MCF7 cells in each of the treatments in different scratches. (K) The mean of Youngs' Modulus values (kpa) of MCF7 cells in treatment with HA and FA

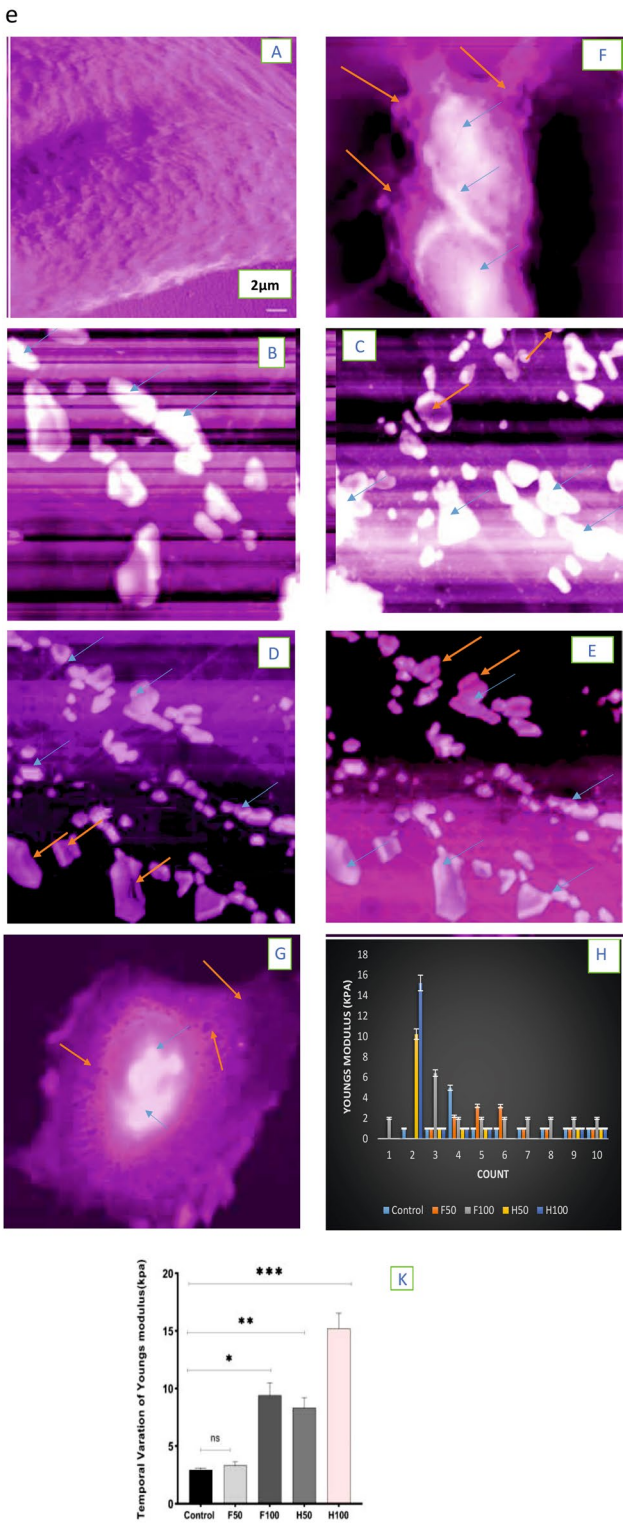

Fig. 4 (continued)

Change in Expression of Bax and Bcl2 Genes in MCF7 Cells

In the current research, the anticancer activity of HA and FA against MCF7 cells was studied by assessing variations in relative gene expression. The changes in relative gene expression were identified through real-time PCR assay. Figure 4c has presented the estimated relative gene expressions after 14 h treatment in concentrations (50,100 µg/mL). There was a significant reduction ($p < 0.05$) in relative gene expression in cured MCF7 cells. As you can see in the figure, the apoptotic gene expression in the HA (100 µg/mL) treatment group was significantly reduced.

Caspase-3 in MCF7Cells Treated with HA and FA

The expressions of the caspase3 gene as the target gene and the GAPDH gene as the reference gene were investigated in 14 h incubation time with real-time PCR. Gene expression analysis was done on treated and non-treated MCF-7 cells after 14 h. Caspase-3 is a vital executioner molecule during the apoptotic process. Numerous studies have revealed the close association of caspase-3 expression and breast cancer. Nevertheless, the prognostic value of caspase-3 expression for patients with breast cancer remains uncertain. Figure 4d has presented the estimated relative gene expressions after 14 h treatment in concentrations (50,100 µg/mL). There was not a significant reduction ($p < 0.05$) in relative gene expression in cured MCF7 cells by FA. As you can see in the figure, the apoptotic gene expression in the HA (100 µg/mL) treatment group was significantly increased. Increasing evidence has shown that down-regulation of caspase-3 is correlated with the development of breast cancer [27, 36]. Several studies reported that caspase-3 expression decreased the likelihood of developing breast cancer [37, 38], while other studies reached the opposite conclusion [39, 40]. Likewise, several studies indicated that caspase-3 expression was significantly correlated with prognosis in breast cancer patients [28, 41], while some studies found the opposite [42, 43]. Generally previous result studies that high caspase-3 expression was significantly associated with a worse prognosis for patients with breast cancer. Moreover, caspase-3 expression is significantly related to the PR and HER-2 status of patients with breast cancer. Therefore, caspase-3 might be a potential biomarker for predicting advanced stage and poor overall survival in breast cancer patients.

Table 2 Results of Cell cycles analysis of the effect of Humic and Fulvic acids (50, 100 µg/mL) on MCF7 Cells at 0,4,8 and 14hrThe analysis was performed based on the Mean ± SD and the *sign indicated that it was significant($P < 0.05$)

Time (h)	Factor	F50	F100	H50	H100
0	G1	61.96 ± 1.9	48.92 ± 1.3	54.97 ± 1.4	57.23 ± 2.8
	S	30.59 ± 2.5	32.57 ± 1.8	34.62 ± 2.3	29.31 ± 1.6
	G2	9.65 ± 1.1	14.32 ± 1.1	7.77 ± 0.8	9.35 ± 1.2
	SubG1	2.01 ± 0.9	8.64 ± 0.4	8.67 ± 0.5	8.6 ± 0.7
4	G1	69.55 ± 2.2	61.84 ± 1.8*	54.94 ± 2.2	72.9 ± 4.1*
	S	18.66 ± 0.8*	25.72 ± 0.6	19.23 ± 1.1*	15.58 ± 1.8*
	G2	8.65 ± 0.3	5.4 ± 0.1*	8.39 ± 0.3	5.4 ± 0.6
	SubG1	5.98 ± 0.1	2.2 ± 1.1*	3.11 ± 2.3	7.03 ± 1.1
8	G1	60.42 ± 1.8	61.41 ± 2.4*	59.41 ± 3.8	59.48 ± 4.5
	S	26.4 ± 0.9	23.12 ± 0.8	25.78 ± 1.2	22.57 ± 1.9
	G2	6.76 ± 0.2	10.79 ± 1.1	6.35 ± 1.1	6.31 ± 0.65
	SubG1	4.3 ± 0.1	5.12 ± 0.45 *	5.2 ± 0.1	7.84 ± 1.1
14	G1	84.22 ± 1.9*	94.08 ± 3.3*	74.79 ± 5.2*	85.36 ± 7.1*
	S	16.57 ± 1.8*	9.42 ± 0.4 *	22.32 ± 3.2	11.96 ± 0.2*
	G2	4.15 ± 0.2	5.08 ± 0.2*	7.45 ± 1.8	7.22 ± 0.5
	SubG1	6.11 ± 0.4	2.06 ± 0.6*	2.59 ± 0.7*	4.59 ± 0.2*

Mechanical Properties

The results of the analysis of the images taken using the software JPK showed that with increasing concentration of drugs (HA and FA), the flexibility of the treated cells decreases. AFM images usually show striations on the topographic surface that reach the dendrites from the cell body. Henderson et al. and Breat et al. reported in 1992 and 2001 that, in AFM topographies, such constructions depend on the subsurface cell actin cytoskeleton [44, 45]. Another study showed that supple surface constructions imaged and recorded by AFM can be actin-based [46]. Thus, the prevalent constructions on cells with notable genetic disparities can be recognized by surface technique (AFM). The center zone of both live MCF-7 cells was investigated using AFM imaging in contact mode (Fig. 4e. A). Probably, the observed filamentous constructions were actin stress fibers because actin structures are the main part of the cytoskeleton localized under the cellular membrane [47]. The pores and apoptotic bodies around the cytoplasmic membrane were observed in cells treated with the HA and FA, shown in Fig. 4eB–E. The blue and brown arrows indicate the apoptotic bodies and visible pores on the surface of cells. The Young modulus values were in control, 2.93 ± 0.016 kpa in FA, 50 µg/ mL,3.32 ± 0.032 kpa in FA, 100 µg/mL, 9.41 ± 3.51 kpa in HA, 50 µg/mL and 100 µg / mL8.39 ± 0.9 and 15.32 ± 5.32 treated cells, as shown in Table 3, Fig. 4e, H and K. The Young's modulus value in the cells cured with HA (100 µg/mL), was more in comparison with the control group. Also, there was a direct relationship between the adhesion force and the elastic modulus. The highest value of the cell-to-cell adhesion force belonged to the cells treated with HA (100 µg/mL). We showed that treated cells were less stiff than normal MCF-7 cells because there were reinforced filamentous structures underneath the cell membrane for backing the MCF7 cells, not for the cured cells (Fig. 4e).

Discussion

Recently, the consumption of herbs and natural products to prevent illnesses and preserve public health has become popular. Several reports confirm the anti-inflammatory, antimicrobial or antioxidant properties and apparent neuroprotective effects of FA [8–10]. It is indicated that HA can protect humans against cancers and cancer-causing viruses [48]. The association between apoptosis and cancer has been affirmed by previous researches. Also, several researchers have proposed that the neoplastic transformation, progression, and metastasis processes involve changes in the usual apoptotic path [49]. Yen et al. and yang et al. has stated that HA can cause the induction of apoptosis in HL-60 and HIT-T15 cells [31, 50]. There was notable cytotoxicity of HA in MCF7 cells after the exposure times and the statistical (DOE) and laboratory results confirmed it (Figs. 1, 2, 3 Table 1). Scholars have described apoptosis as a very regulated process, in which a cascade of molecular events is activated causing cell necrosis. We showed the induction of HA apoptosis at concentrations of IC50 and 100 µg/mL, which was similar to the previously reported results [33, 51]. Also, several studies reported that Bax genes and Bcl-2 have crucial roles in the cells apoptosis [52, 53]. An association was observed between the increment of FA and HA-induced apoptosis and the increment of Bax protein levels, which heterodimerizes with Bcl-2 and thereby inhibits it, Fig. 4c. Along with this change, we see a decrease in

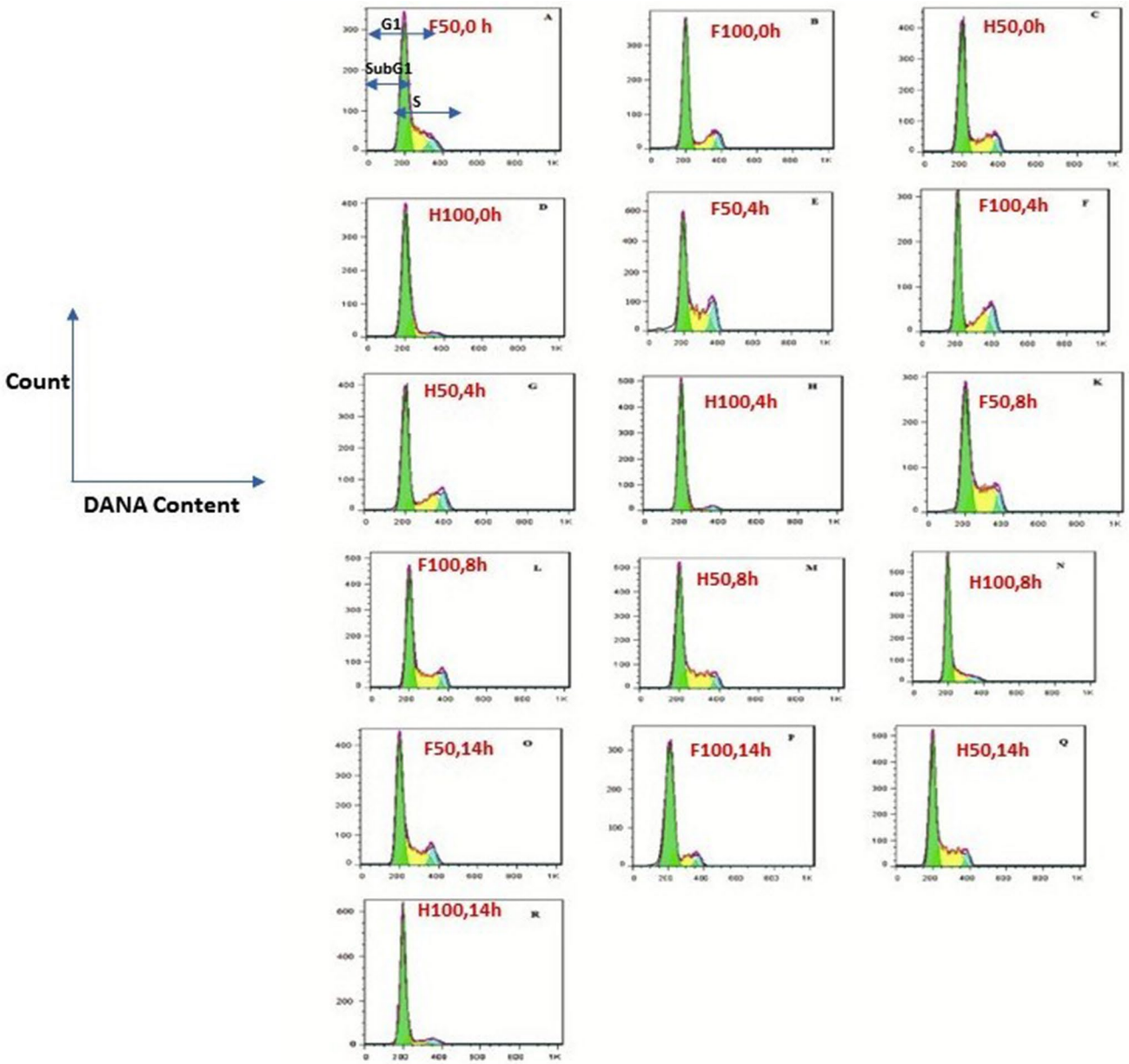

Fig. 5 Cell cycle results at different times and concentrations of 0.50 to 100 µg/mL FA and HA Images **A**–**D**. 0 h, Images (**E**–**H**). 4 h, Images (**K**–**N**) .8 h, Images (**O**–**R**). 14 h

Table 3 Atomic force microscopy data analysis

Compounds	Mean Young's Modulus value(kpa) ± SD	Mean Adh. Force (pN) ± SD	Mean Z pulling (µm) ± SD	p	P[1]
Control	2.93 ± 0.016	148 ± 7.2	1.56 ± 0.06	–	–
FA 50	3.32 ± 0.032	193 ± 6.3	1.32 ± 0.01	0.062	0.015*
FA 100	9.41 ± 3.51	210 ± 7.1	1.82 ± 0.02	0.033*	< 0.001*
HA 50	8.32 ± 0.9	252 ± 11.3	1.91 ± 0.05	0.01*	0.017*
HA 100	15.23 ± 5.32	298 ± 13.8	2.56 ± 0.09	< 0.001*	0.01*

Youngs modulus and mean adhesion force values of MCF7 cells.**p** and **p[1]**: comparsion of The mean of Youngs' Modulus in treatment groups with control

**p* value 0.05

expression in gene Bcl-2, though. The current research has confirmed that HA and FA might change the ratio of Bax and Bcl-2 and, accordingly, causes the apoptosis of MCF7 cells, as Hsin Ling Yang et al. pointed out [31].The expression levels of the *caspase-3* gene have been measured in different cancer cell lines. The treatment of Hone1, AGS, HCT-116, and CL1-0 cell lines with Carla extract led to increase in *caspase-3* activity (two-fold changes) [54]. In this study, we present evidence demonstrating that HA-induced apoptosis of MCF7 cells is mediated by increased cytosolic translocation of cytochrome c, activation of caspase 3, and degradation of PARP (Fig. 4d). many papers have reported that internucleosomal DNA fragmentation is not essential in apoptotic cell death, and that some necrotic cell death is accompanied by internucleosomal DNA fragmentation, suggesting that this fragmentation may not be sufficient as an indicator of apoptotic cell death in MCF7 cell line. it is clear, however, that the central mechanism of apoptosis is evolutionary conserved, and that caspase activation is an essential step in these complex apoptotic pathways. Our data, therefore, provide additional important evidence that HA-induced cell death is apoptosis related as Hsin Ling Yang et reported in HL-60 cells [29]. But we did not reach the right conclusion about FA. Liang et al. showed that by producing superoxide anion could mediate the HA-induced oxidative injury in cultured articular chondrocytes of rabbit [55, 56]. Additionally, Visser et al. indicated that HA and FA obtained from podzol-instigated respiration in liver mitochondria of rats led to the production of intracellular reactive oxygen species [57]. Based on previous findings, we guess that oxidative stress may mediate apoptosis in MCF7 cells induced by the FA and HA in the present research. The results of current research showed that HA and FA exert anti-proliferative and growth prevention performance in MCF7 cells. Moreover, in the present research, the biochemical and ultrastructural characteristics indicated by dying cells were apoptosis characteristics. Just like it has been indicated by cell viability reduction, related to chromatin condensation, and internucleosomal DNA fragmentation. There are still ambiguities about the therapeutic effect of HA on cancer, but reports such as that L.u.et.al; indicated that the neoplastic transformation of mouse epidermal JB6 cells was increased by the HA noncytotoxic concentrations [58]. According to the HA structure, it showed that this compound produced superoxide anion and depleted the glutathione and several antioxidant enzymes [51, 59]. According to the study of Ting et al., HA inhibits cell proliferation through ROS and apoptosis induction [23]. AFM is used to study the mechanical features and dynamics of intact cells related to the various cellular events, including ageing, locomotion, differentiation, cell pathology, and physiological activation and electromobility. In this study, the examination of cells by atomic force microscopy showed that the most values of Young's modulus and cell–cell adhesion force were in the cells cured by HA. Aligned with our study, many articles have indicated that increasing malignancy led to a reduction of Young's modulus values. Due to the less adhesion potential, the malignant cells are more flexible, which can be because of changing the actin fibers organization and varying the cytoplasmic pressure and density. Also, the cell will be softer due to cell membrane collapse [30, 60, 61].

Conclusions

In conclusion, we observed more anticancer and effective cytotoxic activity of the HA against MCF7 cells. We found that HA and FA can induce apoptosis, and reduce gene expression in cured MCF7 cells. However, we observed HA was more efficient in inducing apoptosis in MCF7 cells. We have seen the dose-dependent behavior of HA in increasing the cell population in phase Sub–G_1. Using the HA and FA increased the elastic modulus values and cell–cell adhesion forces and a dose-dependent manner was confirmed. The high regression coefficient between the predicted values and experimental values of the % Cell viability indicated that the model was successful in correlating the response to the studied parameters.

Acknowledgements We thank the Cellular and Molecular Research Center of the University of Medical Sciences and the Department of Chemistry and Simulation Center of Qazvin Imam Khomeini International University.

Author contributions All authors have approved the submitted version, besides. LZ: Conceptualization, data curation, interpretation of data and writing. NG, GRB: Conceptualization, interpretation of data. BP: interpretation of data and writing, SAH: statistical analysis. All authors have agreed to be personally acountable for their contributions and ensure that all questions were appropriately investigated, resolved and the resolution documented in the literature. All authors read and approved the final manuscript.

Funding Not applicable.

Data Availability The datasets used and/or analysed in the present research are accessible through the corresponding author on reasonable demand.

Declarations

Conflict of interest The authors acknowledge that they have no competing interests.

Consent for publication Not applicable.

Ethical Approval Not applicable.

References

1. Sak, K.: Site-specific anticancer effects of dietary flavonoid quercetin. Nutr. Cancer **66**, 177–193 (2014)
2. Khan, F., et al.: Molecular targets underlying the anticancer effects of quercetin: an update. Nutrients **8**, 529 (2016)
3. Calvo, P., Nelson, L., Kloepper, J.W.: Agricultural uses of plant biostimulants. Plant Soil **383**, 3–41 (2014)
4. Hartenstein, R.: Sludge decomposition and stabilization. Science **212**, 743–749 (1981)
5. Burges, N., Hurst, H., Walkden, B.: The phenolic constituents of humic acid and their relation to the lignin of the plant cover. Geochim. Cosmochim. Acta **28**, 1547–1554 (1964)
6. Ay, F.: Hümik asit ve hümik asit kaynaklarının jeolojik ve ekonomik önemi. Cumhuriyet Üniversitesi Fen Fakültesi Fen Bilimleri Dergisi. **36**, 28–51 (2015)
7. Choudhry, G. G.: Humic substances: Part structural aspects. (1981).
8. Wang, C., Wang, Z., Peng, A., Hou, J., Xin, W.: Interaction between fulvic acids of different origins and active oxygen radicals. Sci. China **39**, 267–275 (1996)
9. Motojima, H., et al.: Properties of fulvic acid extracted from excess sludge and its inhibiting effect on β-hexosaminidase release. Biosci. Biotechnol. Biochem. **73**, 2210–2216 (2009)
10. Van Rensburg, C., Van Straten, A., Dekker, J.: An in vitro investigation of the antimicrobial activity of oxifulvic acid. J. Antimicrob. Chemother. **46**, 853–854 (2000)
11. Jooné, G.K., van Rensburg, C.E.J.: An in vitro investigation of the anti-inflammatory properties of potassium humate. Inflammation **28**, 169–174 (2004)
12. Krzemiński, T.F., et al.: Angiogenesis and cardioprotection after TNFα-inducer-Tolpa Peat Preparation treatment in rat's hearts after experimental myocardial infarction in vivo. Vascul. Pharmacol. **43**, 164–170 (2005)
13. Aykac, A. *et al.* in *Multidisciplinary digital publishing institute proceedings.* 1565.
14. Huang, W.-S., et al.: Fulvic acid attenuates resistin-induced adhesion of HCT-116 colorectal cancer cells to endothelial cells. Int. J. Mol. Sci. **16**, 29370–29382 (2015)
15. Kabel, A.M., F. H. B.: Breast cancer: insights into risk factors, pathogenesis, diagnosis and management. J. Cancer Res. Treat **3**(2), 28–33 (2015)
16. Akhtar, S.J., et al.: Phytochemicals for breast cancer therapy: current status and future implications. Curr. Cancer Drug Targets **15**, 116–135 (2015)
17. Yamazaki, S., Sakakibara, H., Takemura, H., Yasuda, M., Shimoi, K.: Quercetin-3-O-glucronide inhibits noradrenaline binding to α2-adrenergic receptor, thus suppressing DNA damage induced by treatment with 4-hydroxyestradiol and noradrenaline in MCF-10A cells. J. Steroid Biochem. Mol. Biol. **143**, 122–129 (2014)
18. Aghapour, F., et al.: Quercetin conjugated with silica nanoparticles inhibits tumor growth in MCF-7 breast cancer cell lines. Biochem. Biophys. Res. Commun. **500**, 860–865 (2018)
19. Kabel, A.M., Baali, F.H.: Breast cancer: insights into risk factors, pathogenesis, diagnosis and management. J. Cancer Res. Treat **3**, 28–33 (2015)
20. Akbas, S.H., Timur, M., Ozben, T.: The effect of quercetin on topotecan cytotoxicity in MCF-7 and MDA-MB 231 human breast cancer cells1. J. Surg. Res. **125**, 49–55 (2005)
21. Karimi, M., Babaahmadi-Rezaei, H., Mohammadzadeh, G.: Effect of silibinin on maspin and ERα gene expression in MCF-7 human breast cancer cell line. Iran. J. Pathol. **12**, 135 (2017)
22. Yang, J., Liu, R.H.: Synergistic effect of apple extracts and quercetin 3-β-D-glucoside combination on antiproliferative activity in MCF-7 human breast cancer cells in vitro. J. Agric. Food Chem. **57**, 8581–8586 (2009)
23. Ting, H.-C., et al.: Humic acid enhances the cytotoxic effects of arsenic trioxide on human cervical cancer cells. Environ. Toxicol. Pharmacol. **29**, 117–125 (2010)
24. Jayasooriya, R.G.P.T., et al.: Fulvic acid promotes extracellular anti-cancer mediators from RAW 2647 cells, causing to cancer cell death in vitro. Int. Immunopharmacol. **36**, 241–248 (2016)
25. Duo, J., Ying, G.-G., Wang, G.-W., Zhang, L.: Quercetin inhibits human breast cancer cell proliferation and induces apoptosis via Bcl-2 and Bax regulation. Mol. Med. Rep. **5**, 1453–1456 (2012)
26. Pant, K., et al.: Mineral pitch induces apoptosis and inhibits proliferation via modulating reactive oxygen species in hepatic cancer cells. BMC Complement. Altern. Med. **16**, 1–10 (2016)
27. Hu, H., Zhou, S., Li, G., Wu, Y., Gao, W.: Expression of caspase 7, caspase 3, survivin in breast neoplasm and their relationship with clinicopathologic factors. J. Modern. Oncol. **15**, 640–642 (2007)
28. O'Donovan, N., et al.: Caspase 3 in breast cancer. Clin. Cancer Res. **9**, 738–742 (2003)
29. Osakabe, M., et al.: Combination of restriction endonuclease digestion with the ΔΔCt method in real-time PCR to monitor etoxazole resistance allele frequency in the two-spotted spider mite. Pestic. Biochem. Physiol. **139**, 1–8 (2017)
30. Pi, J., et al.: Investigation of quercetin-induced HepG2 cell apoptosis-associated cellular biophysical alterations by atomic force microscopy. Scanning. **38**, 100–112 (2016)
31. Yang, H.-L., et al.: Humic acid induces apoptosis in human premyelocytic leukemia HL-60 cells. Life Sci. **75**, 1817–1831 (2004)
32. Tsai, M.L., Yen, C.C., Lu, F.J., Ting, H.C., Chang, H.R.: Environmentally relevant concentration of arsenic trioxide and humic acid promoted tumor progression of human cervical cancer cells: In vivo and in vitro studies. Environ. Toxicol. **31**, 1121–1132 (2016)
33. Pant, K., et al.: Humic acid inhibits HBV-induced autophagosome formation and induces apoptosis in HBV-transfected Hep G2 cells. Sci. Rep. **6**, 34496 (2016)
34. Jayasooriya, R.G.P.T., M. G. D., Chang-Hee Kang, Seungheon Lee, Yung Hyun Choi, Yong Kee Jeong, Gi-Young Kim: Fulvic acid promotes extracellular anti-cancer mediators from RAW2647 cells, causing to cancer cell death in vitro. Int. Immunopharmacol. **36**, 241–248 (2016)
35. Hollville, E., Martin, S.J.: Measuring apoptosis by microscopy and flow cytometry. Curr. Protocols Immunol. **112**(14), 11–14 (2016)
36. Huang, Q., et al.: Caspase 3–mediated stimulation of tumor cell repopulation during cancer radiotherapy. Nat. Med. **17**, 860–866 (2011)
37. Wu, M.-H., Huang, J.-C., Feng, Z.-B.: Expression of ALDH1 protein and its relationship with cell apoptosis and caspase-3 in breast carcinoma. Chin. J. Clin. Exp. Pathol. **7**, 15 (2012)
38. Devarajan, E., et al.: Down-regulation of caspase 3 in breast cancer: a possible mechanism for chemoresistance. Oncogene **21**, 8843–8851 (2002)
39. Engels, C.C., et al.: The prognostic value of apoptotic and proliferative markers in breast cancer. Breast Cancer Res. Treat. **142**, 323–339 (2013)
40. Hayes, D.F., Isaacs, C., Stearns, V.: Prognostic factors in breast cancer: current and new predictors of metastasis. J. Mammary Gland Biol. Neoplasia **6**, 375–392 (2001)
41. Zhou, L., et al.: Novel prognostic markers for patients with triple-negative breast cancer. Hum. Pathol. **44**, 2180–2187 (2013)
42. Blázquez, S. et al.: Caspase-3 and caspase-6 in ductal breast carcinoma: a descriptive study. Histology and histopathology (2006).

43. Végran, F., et al.: Overexpression of caspase-3s splice variant in locally advanced breast carcinoma is associated with poor response to neoadjuvant chemotherapy. Clin. Cancer Res. **12**, 5794–5800 (2006)
44. Henderson, E., Haydon, P., Sakaguchi, D.: Actin filament dynamics in living glial cells imaged by atomic force microscopy. Science **257**, 1944–1946 (1992)
45. Braet, F., de Zanger, R., Seynaeve, C., Baekeland, M., Wisse, E.: A comparative atomic force microscopy study on living skin fibroblasts and liver endothelial cells. Microscopy **50**, 283–290 (2001)
46. Poole, K., Meder, D., Simons, K., Müller, D.: The effect of raft lipid depletion on microvilli formation in MDCK cells, visualized by atomic force microscopy. FEBS Lett. **565**, 53–58 (2004)
47. Lekka, M., et al.: Elasticity of normal and cancerous human bladder cells studied by scanning force microscopy. Eur. Biophys. J. **28**, 312–316 (1999)
48. Kodama, H.: Antitumor effect of humus extract on murine transplantable L1210 leukemia. J. Vet. Med. Sci. **69**, 1069–1071 (2007)
49. Bold, R.J., Termuhlen, P.M., McConkey, D.J.: Apoptosis, cancer and cancer therapy. Surg. Oncol. **6**, 133–142 (1997)
50. Yen, C.-C., et al.: The diabetogenic effects of the combination of humic acid and arsenic: in vitro and in vivo studies. Toxicol. Lett. **172**, 91–105 (2007)
51. Cheng, M.-L., Ho, H.-Y., Huang, Y.-W., Lu, F.-J., Chiu, D.T.-Y.: Humic acid induces oxidative DNA damage, growth retardation, and apoptosis in human primary fibroblasts. Exp. Biol. Med. **228**, 413–423 (2003)
52. Jacobson, M. D., Burne, J. F. & Raff, M. C. (Portland Press Ltd., 1994).
53. Jacobson, M.D., Raff, M.C.: Programmed cell death and Bcl-2 protection in very low oxygen. Nature **374**, 814–816 (1995)
54. Li, C.-J. et al.: Momordica charantia extract induces apoptosis in human cancer cells through caspase-and mitochondria-dependent pathways. Evidence-Based Compl. Altern. Med. **2012** (2012).
55. Liang, H.-J., Tsai, C.-L., Chen, P.-Q., Lu, F.-J.: Oxidative injury induced by synthetic hum1c acid polymer and monomer in cultured rabbit articular chondrocytes. Life Sci. **65**, 1163–1173 (1999). https://doi.org/10.1016/S0024-3205(99)00350-1
56. Tsai, H.-J.L.C.-L., Lu, F.-J.: Oxidative stress induced by humic acid solvent extraction fraction in cultured rabbit articular chondrocytes. J. Toxicol. Environ. Health A **54**, 477–489 (1998)
57. Visser, S.: Effect of humic substances on mitochondrial respiration and oxidative phosphorylation. Sci. Total Environ. **62**, 347–354 (1987)
58. Lu, F.-J., et al.: Promoting neoplastic transformation of humic acid in mouse epidermal JB6 Cl41 cells. Chem. Biol. Interact. **162**, 249–258 (2006)
59. Cheng, M.-L., Ho, H.-Y., Chiu, D.T.-Y., Lu, F.-J.: Humic acid–mediated oxidative damages to human erythrocytes: A possible mechanism leading to anemia in blackfoot disease. Free Radical Biol. Med. **27**, 470–477 (1999)
60. Soufi, L., Farasat, A., Ahmadpour-Yazdi, H., Zolghadr, L., Gheibi, N.: The effects of the esterified Quercetin with omega3 and omega6 fatty acids on viability, nanomechanical properties, and BAX/BCL-2 gene expression in MCF-7 cells. Mol. Biol. Rep. **48**, 5161–5169 (2021)
61. Iturri, J., et al.: Resveratrol-induced temporal variation in the mechanical properties of MCF-7 breast cancer cells investigated by atomic force microscopy. Int. J. Mol. Sci. **20**, 3275 (2019)